

# Serially-Linked Parallel Leg Design for Biped Robots

Ohung Kwon, Jung H. Yoon, Je S. Yeon, and Jong H. Park\*

Dept. of Precision Mechanical Engineering, \*School of Mechanical Engineering  
Hanyang University, Seoul, Korea  
ohung210@hanmail.net \*jongpark@hanyang.ac.kr

## Abstract

In this paper, we propose a biped robot each of whose legs is composed of two 3-DOF parallel platforms that are linked serially. The thigh of each leg consists of a 3-DOF orientation platform and the shank consists of 3-DOF asymmetric parallel platform. The former consists of 3 active linear actuators and 7 passive joints. And the latter consists of two active linear actuators, one active rotational actuator, and 5 passive joints. Also, the active and passive joints are configured to move freely without any kinematic constraints. The effectiveness and the performance of the proposed parallel platforms with some locomotion trajectory are demonstrated in computer simulations. They indicate that the proposed robot can move freely in man-made environment and can be used in many areas including medical applications and welfare where heavy payloads are to be needed.

**Keywords:** parallel link, biped robots, trajectory, sagittal plan, locomotion

## 1 Introduction

The structure of biped robots with serial links requires many complex design in order to reduce the actuator power of each joint using light special materials such as magnesium, and the special processing. And, it needs much cost to lighten link weight of two legs and also has many limitations in control loads of biped robots, thus, carrying goods and pushing a cart.

Therefore, biped robots with parallel mechanisms are proposed as a substitute in order to overcome these problems because this parallel structure possesses an ability to deal with heavy loads.

Some researchers have been working on these parallel mechanisms for biped robots which can walk stably, carry heavy loads, and push a cart [1–5]. They proposed parallel-type biped robots whose legs were composed of links with small inertia and took advantage of the parallel mechanism that have high rigidity in their structure. However, these robots do not look like human beings at all in that they don't have knees, and moreover, do not walk *naturally* as a human does.

Thus, we propose a new parallel mechanism for a three dimensional biped robot, each leg of which is composed of two 3-DOF parallel platforms as a thigh and a shank. These two mechanisms are linked together to form a knee, thus yielding a configuration similar to that of a typical serially-linked leg. One leg consists of a thigh, a 3-DOF parallel platform, and a shank, a 3-DOF asymmetric parallel platform. The thigh consists of three active linear actuators and seven passive joints, and the shank consists of two linear actuator, one rotational actuator, and five passive joints.

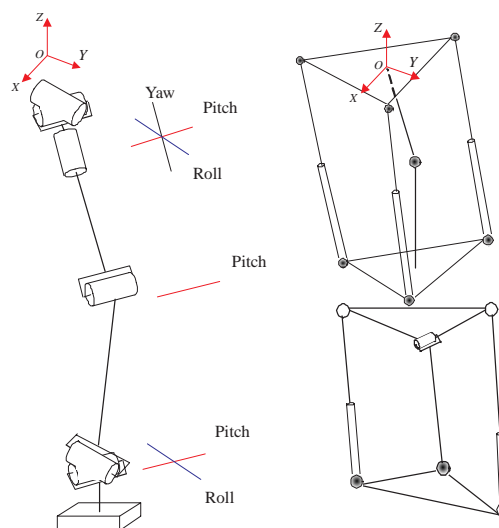


Figure 1: The proposed leg for biped robot with a parallel mechanism shown on the right is designed to have its own knee as a typical leg with a serial link mechanism shown on the left.

This paper is organized as follows: Section 2 describes the detail structure of the new parallel leg for biped robots. Section 3 describes trajectories of parallel biped robot based on GCIPM. The effectiveness of the proposed control algorithms is shown through computer simulations in Section 4, followed by conclusions in Section 5.

## 2 Serially-linked Parallel Leg

Each leg of a typical biped robot consists of 6 links that are connected serially as shown in Fig. 1. It has three joints at the pelvis, that are for roll, pitch, and yaw; one

joint at the knee; two joints at the ankle, for roll and pitch of the foot. Overall structure is very similar to that of a human.

The parallel leg structure proposed in this paper uses parallel mechanisms but at the same time has a knee. To perform the same functionality as a typical 6-DOF serial link leg, we adopted a modified orientational platform for the thigh which has 3 SPS (Spherical-Prismatic-Spherical joint) chains and one chain connected by spherical joint at the center to rotate in the 3-axis direction [7, 8]. And the shank consists of a RS (Rotation-Spherical) chain for the pitch motion, UPU (Universal-Prismatic-Universal) and UPS (Universal-Prismatic-Spherical) chains for the pitch and roll motions at the ankle.

## 2.1 Parallel Mechanism for Thigh

Thigh of human beings can generate 3-DOF rotation motions so that they can walk and run freely. Figure 2 shows a 3-DOF orientation platform used to perform 3-DOF rotations of the thigh similar to the human being's.

In order to analyze the characteristics of this parallel mechanism for the thigh, inverse and forward kinematics have to be computed from geometrical relationships.

For that, two Cartesian coordinate frames,  $A(X, Y, Z)$  and  $B(U, V, W)$ , are attached to the lower and the upper platforms, respectively.

Then, the length between the upper platform, platform B, and the lower platform, platform A, at the  $i$ -th chain can be described by

$$d_i \hat{s}_i = \mathbf{b}_i - \mathbf{a}_i (= \overrightarrow{A_i B_i}) \quad \text{for } i = 1, 2, 3 \quad (1)$$

where  $\hat{s}_i$  is the unit vector in the direction of  $\overrightarrow{A_i B_i}$ , and

$$\begin{aligned} \mathbf{a}_i &= [a_{ix} \ a_{iy} \ a_{iz}]^T = \overrightarrow{OA_i} \\ \mathbf{b}_i &= [b_{ix} \ b_{iy} \ b_{iz}]^T = \overrightarrow{OB_i} \end{aligned}$$

From Eq. 1,

$$\begin{aligned} d_i^2 &= (d_i \hat{s}_i)^T (d_i \hat{s}_i) \\ &= (\mathbf{b}_i - \mathbf{a}_i)^T (\mathbf{b}_i - \mathbf{a}_i) \\ &= \|\mathbf{a}_i\|^2 + \|\mathbf{b}_i\|^2 - 2\mathbf{a}_i^T \mathbf{b}_i, \end{aligned}$$

or

$$d_i = \sqrt{\|\mathbf{a}_i\|^2 + \|\mathbf{b}_i\|^2 - 2\mathbf{a}_i^T \mathbf{b}_i} \quad (2)$$

Next, in order to derive the Jacobian of this platform, loop-closure equation of  $i$ -th chain is described as follows.

$$\overrightarrow{OB_i} = \overrightarrow{OA_i} + \overrightarrow{A_i B_i} \quad (3)$$

Noting that point B only turns about the fixed point O, which results in

$$\dot{\mathbf{b}}_i = \omega_B \times \mathbf{b}_i, \quad (4)$$

where  $\omega_B$  is the angular velocity of platform B, and that the rate change of a vector can be represented by the combination of its change with respect to a rotating coordinate frame, and the cross-product of rotating velocity of the coordinate and the vector, which results in

$$\frac{d}{dt} (d_i \hat{s}_i) = \dot{d}_i \hat{s}_i + \omega_i \times (d_i \hat{s}_i), \quad (5)$$

where  $\omega_i$  is the angular velocity of the  $i$ -th chain, differentiating Eq. 3 with respect to time yields a velocity vector-loop equation:

$$\omega_B \times \mathbf{b}_i = \omega_i \times (d_i \hat{s}_i) + \dot{d}_i \hat{s}_i \quad (6)$$

Pre-multiplying this equation by  $\hat{s}_i^T$ ,

$$\hat{s}_i^T (\omega_B \times \mathbf{b}_i) = \dot{d}_i$$

which can be written as

$$\dot{d}_i = (\mathbf{b}_i \times \hat{s}_i)^T \omega_B. \quad (7)$$

Therefore,

$$\dot{\mathbf{q}} = J_x \omega_B \quad (8)$$

where

$$\begin{aligned} \dot{\mathbf{q}} &= [\dot{d}_1 \ \dot{d}_2 \ \dot{d}_3]^T \\ J_x &= \begin{bmatrix} (\mathbf{b}_1 \times \hat{s}_1)^T \\ (\mathbf{b}_2 \times \hat{s}_2)^T \\ (\mathbf{b}_3 \times \hat{s}_3)^T \end{bmatrix}. \end{aligned} \quad (9)$$

Note that  $J_x$  is the Jacobian matrix for the parallel mechanism, which transforms a end-effector velocity, or task-space velocity, in  $m$ -dimensional space to a joint velocity in  $n$ -dimensional space, and is configuration dependent. Therefore, for design and analysis with various parallel platforms, the Jacobian matrix plays an important role. The Jacobian matrix can be characterized by a measure called Isotropic Index,  $\eta$ , which is defined as the ratios of maximum and minimum singular values of the Jacobian matrix, and depends on the manipulator configuration as well as system parameters such as the length of the links.

$$\eta(J_x) = \frac{\sigma_{\min}(J_x)}{\sigma_{\max}(J_x)} \quad (10)$$

where  $\sigma_{\min}(\cdot)$  and  $\sigma_{\max}(\cdot)$  is the minimum and maximum singular values of a matrix, respectively.

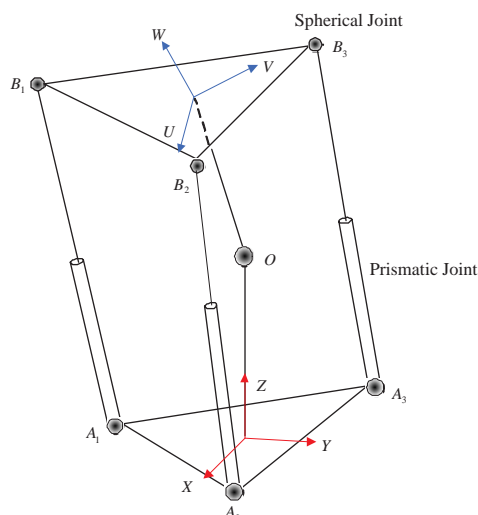


Figure 2: A 3-DOF orientation platform.

Using the Isotropic Index, we determine the optimal configuration of this platform by rotating into the direction of roll, pitch and yaw axis. Firstly, the Isotropic Index has the uniform distribution of the parabolic shape in Fig. 3(a). This configuration is irrelevant to walking motion because it occupies small workspace. Therefore, as shown in Fig. 3(b) and (c), in order to have large displacement along the sagittal plane, the end effector of each chain connected at the corner positions of the upper plate is connected into the corner positions of the lower plate with the asymmetric triangle shape. Also, when the top plate is twisted about 45 degrees into the yaw direction, Fig. 3(c) shows that this platform has larger isotropic index and wider workspace than that of the symmetric arrangement. In short, end-effectors of each chain are arranged at the corner position of the lower platform made into 160-160-40 degrees as shown in Fig. 3(c). And the position of a spherical joint located in the chain's center region is adjusted to maximize the workspace.

## 2.2 Parallel Mechanism for Shank

Swing motion of the shank requires two joints for the pitch motion and one joint for the roll motion. Therefore, we proposed new parallel manipulator, a asymmetric platform, composed of 6-5-4 DOF chains to ensure pitch motion of knees, another pitch and roll motion of ankle instead of 3 symmetrical limbs. There is one joint to make a knee motion on the top plate and two joints to make ankle motion on the base plate such as shown in Fig. 4.

For its kinematic analysis, similarly to the thigh, two Cartesian coordinate systems  $A(X, Y, Z)$  and  $B(U, V, W)$  are attached to the upper platform, platform A, and lower platform, platform B, respectively.

From Fig. 4,

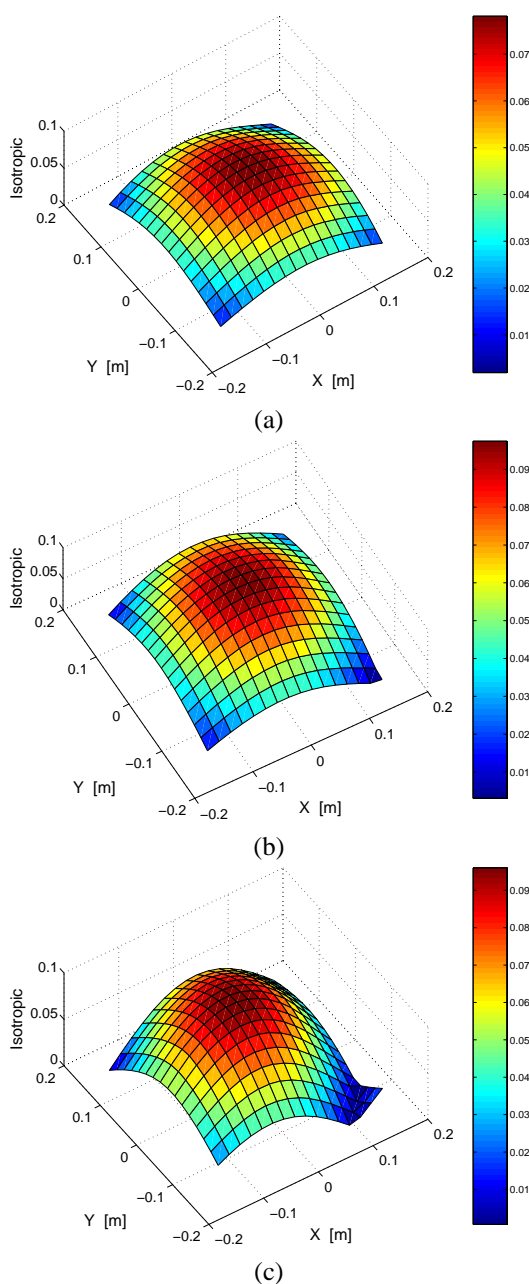


Figure 3: Isotropic index: (a) when end-effectors of each chain are arranged at the corner position of the lower platform made into the regular triangle (120-120-120 degrees) and the upper platform are rotated 45 degrees into the yaw axis. (b) when end-effectors of each chain are arranged at the corner position of the lower platform made into the asymmetric triangle (140-140-80 degrees) and the upper platform are rotated 45 degrees into the yaw axis. (c) when end-effectors of each chain are arranged at the corner position of the lower platform made into the asymmetric triangle (160-160-40 degrees) and the upper platform are rotated 45 degrees into the yaw axis.

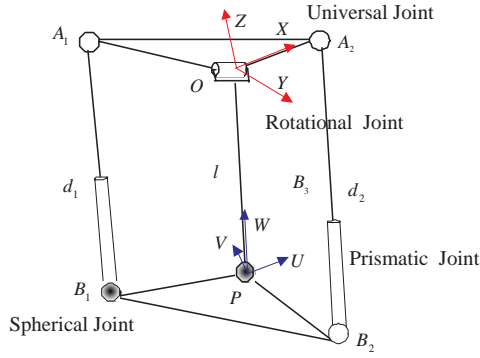


Figure 4: A 3-DOF asymmetric platform.

$$d_i \hat{\mathbf{s}}_i = \mathbf{p} + \mathbf{b}_i - \mathbf{a}_i \quad \text{for } i = 1, 2 \quad (11)$$

where  $d_i$  denotes the length of the  $i$ -th chain and  $\hat{\mathbf{s}}_i$  is the unit vector in the direction of  $\overrightarrow{A_i B_i}$ .

$$\begin{aligned} \mathbf{p} &= \overrightarrow{OP} \\ \mathbf{a}_i &= [a_{ix} \ a_{iy} \ a_{iz}]^T = \overrightarrow{OA_i} \\ \mathbf{b}_i &= [b_{iu} \ b_{iv} \ b_{iw}]^T = \overrightarrow{PB_i} \end{aligned}$$

If the orientation of the upper platform is known, the  $i$ -th chain length,  $d_i$  is obtained by the inverse kinematics. Thus,

$$\begin{aligned} d_i^2 &= \|\mathbf{a}_i\|^2 + \|\mathbf{p} + \mathbf{b}_i\|^2 - 2\mathbf{a}_i^T(\mathbf{p} + \mathbf{b}_i) \\ d_i &= \sqrt{\|\mathbf{a}_i\|^2 + \|\mathbf{p} + \mathbf{b}_i\|^2 - 2\mathbf{a}_i^T(\overrightarrow{OP} + \mathbf{b}_i)} \quad (12) \end{aligned}$$

A loop-closure equation for the  $i$ -th chain, Eq. 11, in order to obtain the Jacobian matrix of this system can be written as

$$d_i \hat{\mathbf{s}}_i + \mathbf{a}_i = \mathbf{p} + \mathbf{b}_i \quad (13)$$

If taking the derivative of Eq. 13 with respect to time yields a velocity vector-loop equation and dot-multiplying both sides by  $\hat{\mathbf{s}}_i$ ,

$$\hat{\mathbf{s}}_i^T \mathbf{V}_p + (\mathbf{b}_i \times \hat{\mathbf{s}}_i)^T \boldsymbol{\omega}_p = \dot{d}_i \quad (14)$$

where  $\mathbf{V}_p$  is determined by the pitch joint of the upper platform and the angular velocity of the lower plate,  $\boldsymbol{\omega}_p$ , is written in terms of the Euler angles and the body-fixed  $\mathbf{U}$  and  $\mathbf{V}'$  unit vectors. Thus,

$$\boldsymbol{\omega}_p = \dot{\alpha} \mathbf{U} + \dot{\beta} \mathbf{V}' \quad (15)$$

where  $\mathbf{U}$  and  $\mathbf{V}'$  are not orthogonal. And  $\alpha$  and  $\beta$  are the rotational angles of the  $\mathbf{U}$  axis direction and the  $\mathbf{V}'$  axis direction in the lower plate, respectively. Also,

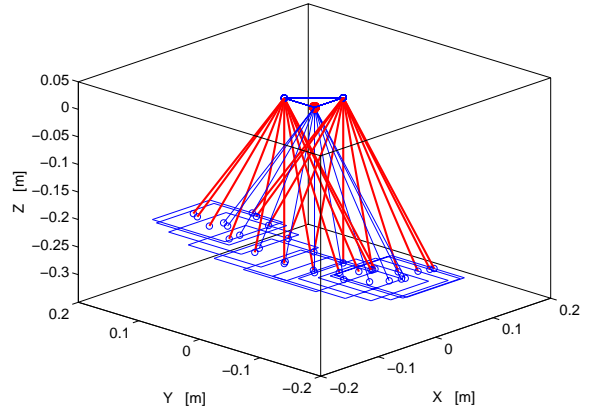


Figure 5: A asymmetric platform in the sagittal plane.

$$\mathbf{U} = \begin{bmatrix} 1 \\ 0 \\ 0 \end{bmatrix} \quad \text{and} \quad \mathbf{V}' = \begin{bmatrix} 1 & 0 & 0 \\ 0 & \cos(\alpha) & -\sin(\alpha) \\ 0 & \sin(\alpha) & \cos(\alpha) \end{bmatrix} \begin{bmatrix} 0 \\ 1 \\ 0 \end{bmatrix}$$

Therefore,

$$\boldsymbol{\omega}_p = \dot{\alpha} \mathbf{U} + \dot{\beta} \mathbf{V}' = \begin{bmatrix} \dot{\alpha} \\ \dot{\beta} \cos(\alpha) \\ \dot{\beta} \sin(\alpha) \end{bmatrix} \quad (16)$$

If selecting the axis of the rotational joint into the X direction in the upper platform and defining the rotational joint angle into  $\theta$ ,

$$\mathbf{V}_p = \begin{bmatrix} 0 \\ l \cos(\theta) \dot{\theta} \\ -l \sin(\theta) \dot{\theta} \end{bmatrix} \quad (17)$$

Thus, the Jacobian of this platform is obtained by combining Eq. 16 and Eq. 17:

$$\mathbf{V}_p = \begin{bmatrix} 0 \\ l \cos(\theta) \\ -l \sin(\theta) \end{bmatrix} \dot{\theta}, \quad \text{and} \quad \begin{bmatrix} \dot{\alpha} \\ \dot{\beta} \end{bmatrix} = J_{as} \begin{bmatrix} \dot{d}_1 \\ \dot{d}_2 \end{bmatrix}$$

where  $J_{as}$  is the Jacobian matrix of the asymmetric platform.

We simulated with the inverse kinematics to prove the appropriation of this asymmetric platform. In general, the lower plate of a symmetric parallel platform can not be moved in parallel with its upper plate when its upper plate is fixed. But, the lower plate of a asymmetric platform moves in parallel with the ground as shown in Fig. 5.

In this paper, a leg of parallel biped robots has the whole structure serially connected both a 3-DOF orientation platform for thigh and a 3-DOF asymmetric platform for shank as shown in Fig. 6.

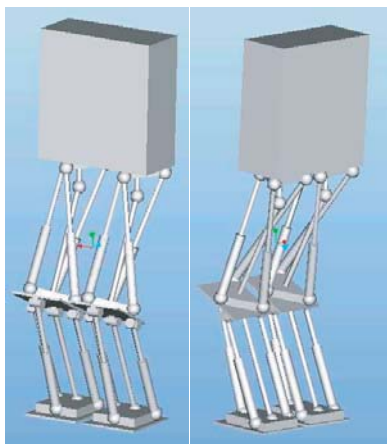


Figure 6: The proposed 12-DOF parallel-linked biped robot.

### 3 Trajectory Generation for Parallel Mechanism

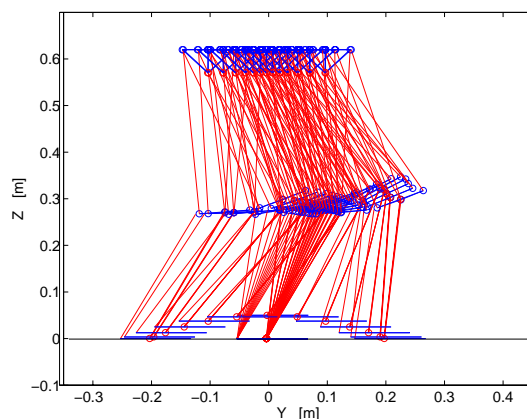
In this paper, we applied trajectories obtained from the modified GCIPM (Gravity-Compensated Inverted Pendulum Mode) [6] for the proposed parallel mechanism in the sagittal plane. The GCIPM is based on a simple biped model which consists of two particles, one for the base link and the other for the free leg. It is from the observation that the most weight of the biped robot is concentrated around its base link and that the free leg sometimes in locomotion moves a far from the base link, its inertia becoming significant. Therefore, trajectories in the sagittal plane are derived from the assumption that the ZMP(Zero Moment Point) exists at the foot's center of supporting leg. And, we applied the LIMP(Linear Inverted pendulum mode) in the lateral plane. As a result, GCIPM and LIPM are applied and divided into trajectories for each upper and lower plate with respect to two knees and feet because two parallel platforms are connected serially.

Table 1: Locomotion parameters for a biped robot.

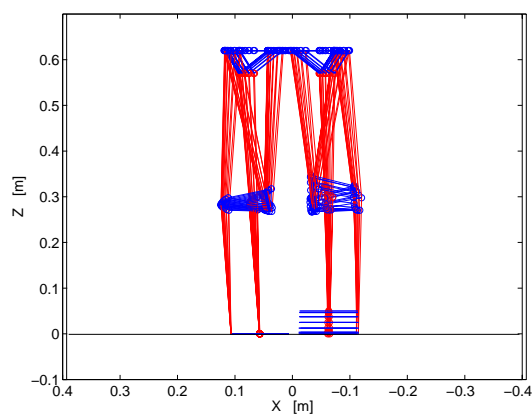
Parameters	Symbol	Dimension
Step Time	T	0.5 s
Hip Height	$H_z$	0.62 m
Stride	S	0.2 m
Max. Foot Height	$h_f$	0.05 m

### 4 Simulations

The effectiveness and the performance of proposed parallel mechanism are shown in computer simulations. The parameters used in computer simulations is shown in Table 1. And the length of the shank and thigh parts are 0.3m, respectively. Assume that each phase is com-



(a)



(b)

Figure 7: Motion of a parallel biped robot in the sagittal and lateral plane.

posed of single support phases, the supporting leg is fixed on the ground and impact force does not exist.

Simulation results of 3-dimensional locomotion of a biped robot with the desired trajectory are shown in Fig. 7 and 9 when its right foot is fixed on the ground and its left foot swings freely. And Fig. 8 shows rotation motions with respect to hip, knee and foot part of serially connected parallel biped robots such as the serial biped robots consisted of one joint for the yaw motion, three joints for the pitch motion, and two joints for the roll motion. This biped robot with parallel structure executes the same performance and role as previous serial biped robots with natural motion of knees. Finally, Analyzing the load exerting on each leg from the static motion analysis, we can conclude that less torque is necessary on the active joints than that of serial biped robots. And a total weight of each leg is expected to be lighter than serial linked leg.

### 5 Conclusion

In this paper, we designed new parallel mechanism of a 3 dimensional biped robot whose each leg is composed of two 3-DOF parallel platforms linked serially to compensate the defect of serial-type biped robot and simu-

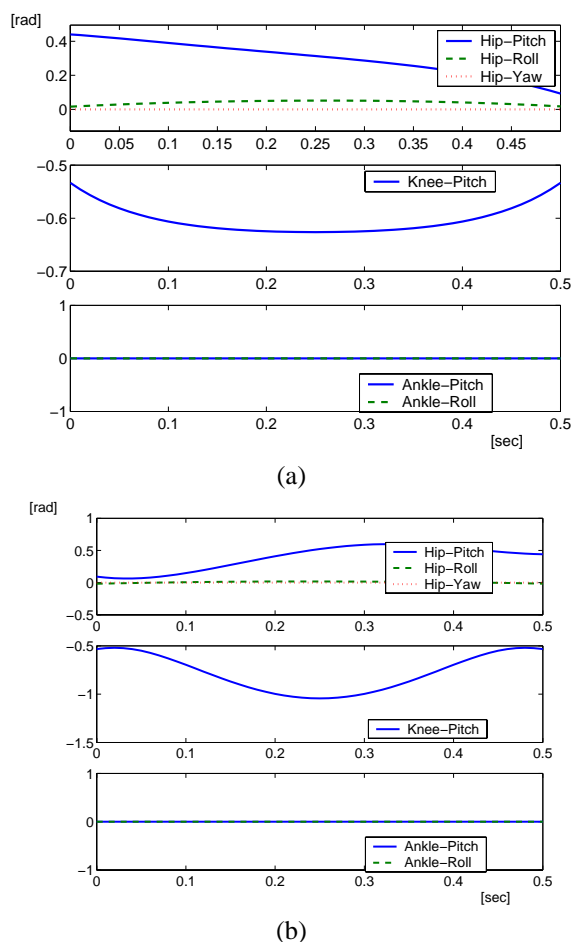


Figure 8: Rotation trajectories with respect to the hip, the knee and the foot of the serially connected parallel biped robot for (a) the right leg and (b) the left leg.

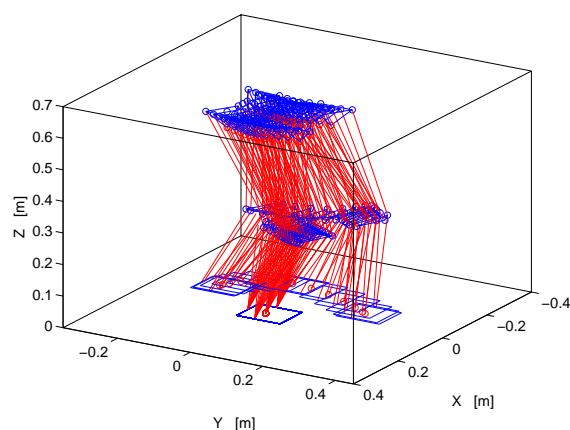


Figure 9: 3D trajectories for a biped robot with two parallel legs.

lated its locomotion with gait trajectories based on the modified GCIPM. The propriety and various possibility of proposed parallel-type model is confirmed through computer simulations. This parallel mechanism in locomotion looks like human legs in locomotion and has

many various application fields such as medical, welfare and entertainment.

## 6 Acknowledgment

This work was supported by Korea Research Foundation Grant (KRF-2003-041-D00056).

## References

- [1] M. Morisawa, T. Yakoh, T. Murakami and K. Ohnishi, "An Approach to Biped Robot with Parallel Mechanism," Proc. of Int. Workshop on Advance Motion Control, pp. 537–541, 2000.
- [2] M. Morisawa, T. Yakoh, T. Murakami and K. Ohnishi, "A Comparison Study Between Parallel and Serial Linked Structures in Biped Robot System," Proc. of Conf. of the IEEE Industrial Electronics Society, pp. 2614–2617, 2000.
- [3] R. Sellaouti, A. Konno, and F. B. Ouedzou, "Design of a 3 DOFs Parallel Actuated Mechanism for biped hip joint," Proc. of IEEE Int. Conf. on Robotics and Automation, pp. 1161–1166, 2002.
- [4] Y. Sugahara, T. Endo, H. O. Lim and A. Takanishi, "Design of a Battery-powered Multi-purpose Bipedal Locomotor with Parallel Mechanism," Proc. of IEEE/RSJ Int. Conf. on Intelligent Robots and Systems, pp. 2658–2663, 2002.
- [5] Y. Sugahara, T. Endo, H. O. Lim and A. Takanishi, "Realization of Stable Dynamic Walking by a Parallel Bipedal Locomotor on Uneven Terrain Using a Virtual Compliance Control," Proc. of IEEE/RSJ Int. Conf. on Intelligent Robots and Systems, pp. 595–600, 2003.
- [6] J. H. Park and K. D. Kim, "Biped Robot Walking Using Gravity-Compensated inverted Pendulum Mode and Computed-Torque Control," Proc. of IEEE Int. Conf. on Robotics and Automation, pp. 3528–3533, 1998.
- [7] L. W. Tsai, "Robot Analysis : The Mechanics of Serial and Parallel Manipulators," John Wiley and Sons, 1999.
- [8] S. Joshi and L. W. Tsai, "A Comparison Study of Two 3-DOF Parallel Manipulators: One With Three and the Other With Four Supporting Legs," Proc. of IEEE Trans. on Robotics and Automation, Vol. 19, no. 2, pp. 200–209, 2003.
- [9] J. P. Merlet, "Parallel Robots," Kluwer Academic Publishers, 2000.